

OPTIMIZATION OF CONTRAST SENSITIVITY AND SPECIFICITY OF QUADRATIC ULTRASONIC IMAGING

Mamoun F. Al-Mistarihi

Electrical Engineering Department, Faculty of Engineering, Jordan University of Science and Technology
Irbid 22110, Jordan
phone: +(962) 2-7201000, fax: +(962) 2-7095018, e-mail: mistarihi@just.edu.jo

ABSTRACT

We present a new algorithm of post-beamforming second order Volterra filter (SOVF) for deriving the quadratic kernel based on the convolution of the singular modes quadratic kernels which give the highest contrast-to-tissue ratio (CTRs) to extract quadratic components from ultrasound contrast agent (UCA) nonlinear echoes with single transmission. The new algorithm leads to reduction of tissue component and increase the specificity while optimizing the sensitivity to the UCA. The algorithm is demonstrated experimentally using images from in vivo kidney after bolus injection with UCA. Illustrative images of the kidney of a juvenile pig were obtained before and after infusion of contrast agent (SonoVue, Bracco, Geneva, Switzerland) at various concentrations. The imaging results given in this paper indicate that a signal processing approach to this clinical challenge is feasible.

Index Terms - post-beamforming, ultrasound contrast agent, contrast-to-tissue ratio, second order Volterra filter

1. INTRODUCTION

Microbubble ultrasound contrast agents (UCA) are being investigated for use in clinical imaging applications for tissue function and for targeted therapeutic applications. The objective is to detect minute concentrations of UCA in the microvasculature during ultrasonic exams thus providing a view of the perfusion in the tissue. This functional form of ultrasonic imaging is seen an important component for the continued use of ultrasound as a medical imaging modality. For example, many tumors without distinguishing characteristics on conventional ultrasound have characteristic blood perfusion patterns that allow for easy detection if a perfusion sensitive imaging is available.

Interaction between microbubbles UCAs and acoustic wave result in nonlinear harmonic echo generation. This phenomenon can be exploited to enhance the echoes from the microbubbles and, therefore, reject fundamental components resulting largely from tissue. Imaging techniques based on nonlinear oscillations have been designed for separating and

enhancing nonlinear UCA echoes from a specified region of interest within the imaging field, including second harmonic (SH) imaging and pulse inversion (PI) Doppler imaging [1]. The SH imaging employs a fundamental frequency transmit pulse and produces images from the second harmonic component of received echoes by using a second harmonic bandpass filter (BPF) to remove the fundamental frequency. In order to increase UCA detection sensitivity in the limited transducer bandwidth condition, spectral overlap between fundamental and second harmonic parts need to be minimized by transmitting narrow-band pulses resulting in an inherent tradeoff between contrast and spatial resolution. In PI imaging a sequence of two inverted acoustic pulses with appropriate delay is transmitted into tissue. Images are produced by summing the corresponding two backscattered signals. In the absence of tissue motion, the resulting sum can be shown to contain only even harmonics of the nonlinear echoes. The PI imaging overcomes the tradeoff between contrast and spatial resolution because it utilizes the entire bandwidth of the backscattered signals. As a result, superior spatial resolution can be achieved when compared with SH imaging. However, the subtraction process results in significant reduction of signal to noise as the harmonics are typically 20 - 30 dB or more below the (cancelled) fundamental component.

The SOVF-based quadratic kernels provide high sensitivity to harmonic echoes comparable to PI with a significant increase in dynamic range due to inherent noise rejection of quadratic filtering [2]. An algorithm for deriving the coefficients of the kernel using singular values decomposition (SVD) of a linear and quadratic prediction data matrix was proposed and experimentally validated in [3]. Imaging results and comparisons with SH and PI images have shown that quadratic imaging is superior to SH and compares favorably with PI without the need for multiple transmissions. However, due to reliance on linear and quadratic prediction, the quadratic kernel has sensitivity to the fundamental that limits its ability to detect UCA in the microvasculature.

In this paper, we present a new algorithm of post-beamforming second order Volterra filter (SOVF) for deriving the quadratic kernel based on the convolution of the singular modes quadratic kernels which give the highest CTRs leading to images with significant improvement in contrast between the UCA and surrounding tissue. We demonstrate this improvement using in-vivo data acquired using real-time commercial ultrasound scanner. Compared with the PI image

processed from the same RF data, the quadratic images show a significant increase in harmonic sensitivity, reduction in noise levels, and comparable performance in terms of both contrast and spatial resolution without the sacrifice of imaging frame rates. Similar results were obtained from imaging flow phantom under a variety of exposure conditions and UCA concentration levels. Implications of this approach on new forms of functional ultrasound imaging are discussed.

2. THEORY

2.1 MNLS Estimation of SOVF Coefficient

The algorithm in this section is based on [2-3], which have shown the validity of a SOVF as a model for pulse-echo ultrasound data from tissue mimicking media. The response of a quadratically nonlinear system with memory $\hat{y}(n+1)$, can be predicted by a second order Volterra model of m past values as follows:

$$\hat{y}(n+1) = \sum_{i=0}^{m-1} y(n-i)h_L(i) + \sum_{j=0}^{m-1} \sum_{k=j}^{m-1} y(n-j)y(n-k)h_Q(j,k) \quad (1)$$

where $h_L(i)$ and $h_Q(j,k)$ are the linear and quadratic filter coefficients respectively. It is easy to see that (1) is a nonlinear equation in terms of the beamformed input data. However, it is a linear equation in terms of the unknown filter coefficients (i.e., linear and quadratic Volterra kernels) $h_L(i)$ and $h_Q(j,k)$.

Hence, (1) can be rewritten in vector form:

$$\hat{y}(n+1) = Y^T(n)H \quad (2)$$

where past data vector $Y(n)$ is defined at time n as:

$$Y(n) = [y(n), y(n-1), y(n-2), \dots, y(n-m+1), y^2(n), y(n)y(n-1), \dots, y^2(n-m+1)]^T$$

and the filter coefficient vector H is defined as:

$$H = [h_L(0), h_L(1), h_L(2), \dots, h_L(m-1), h_Q(0,0), h_Q(0,1), \dots, h_Q(m-1, m-1)]^T$$

Note that m is the system order, N is the total number of filter coefficients [3], which is equal to $(m^2 + 3m)/2$ assuming symmetrical quadratic kernels (i.e., $h_Q(j,k) = h_Q(k,j)$), and superscript T is the transpose of a vector or a matrix. Similarly, $\hat{y}(n+2), \hat{y}(n+3), \dots, \hat{y}(n+m)$ can be represented in the form of (2) and expressed in a matrix form. A system of linear

equations is formed in order to find filter coefficients as follows:

$$F = GH \quad (3)$$

where the vector F and the data matrix G are:

$$F = [y(n+1), y(n+2), \dots, y(n+L)]^T$$

$$G = [Y(n), Y(n+1), \dots, Y(n+L-1)]^T$$

where L is the number of linear equations (observations). Using a segment of the RF data, a system of linear equations are formed and solved for elements of the quadratic kernel. Details of the algorithm to determine the quadratic kernel that provide maximum contrast enhancement have been described in [2-3].

In this paper, instead of using just one singular mode, we use a solution based on the convolution of the singular modes quadratic kernels which give the highest CTRs. The new algorithm shows that it is more efficient than the previous ones in terms of the enhanced reconstructed image and the CTR values. A two-dimensional (2D) autocorrelation is performed on (h_{qconv}) to alleviate ringing effects of the quadratic kernels, where (h_{qconv}) is the quadratic kernel resulting from the convolution of the singular modes quadratic kernels which give the highest CTRs. We use 2D autocorrelation twice in this paper. Therefore, the 2D autocorrelation of the quadratic kernel (h_{qconv}) , is given by:

$$Q = (h_{qconv} \otimes h_{qconv}) \otimes (h_{qconv} \otimes h_{qconv}) \quad (4)$$

where Q represents the quadratic kernel resulting from 2D autocorrelation of the quadratic kernel (h_{qconv}) twice and “ \otimes ” denotes the operation of 2D correlation.

2.2 Quadratic Images

From the standard B-mode image, after a UCA region and a tissue region are defined for the CTR computation, a segment of RF data from an axial line is selected to form a system of linear equations. The SVD of the G matrix is computed, the filter coefficients for each singular mode of the G matrix are determined and the corresponding CTRs are computed. The quadratic kernel (h_{qconv}) is computed by convolving the singular modes quadratic kernels which give the highest CTRs and a 2D autocorrelation is performed twice. The quadratic image is produced by applying the quadratic filter coefficients of Q to the beamformed RF data throughout the standard B-mode image to estimate the quadratic component

$$\hat{y}_Q(n+1) = \sum_{j=0}^{P-1} \sum_{k=j}^{P-1} y(n-j)y(n-k)Q(j,k) \quad (5)$$

where P is the size of the Q matrix which depends on the number of singular modes used to compute (h_{qconv}) .

A flowchart of this algorithm is shown in Fig. 1.

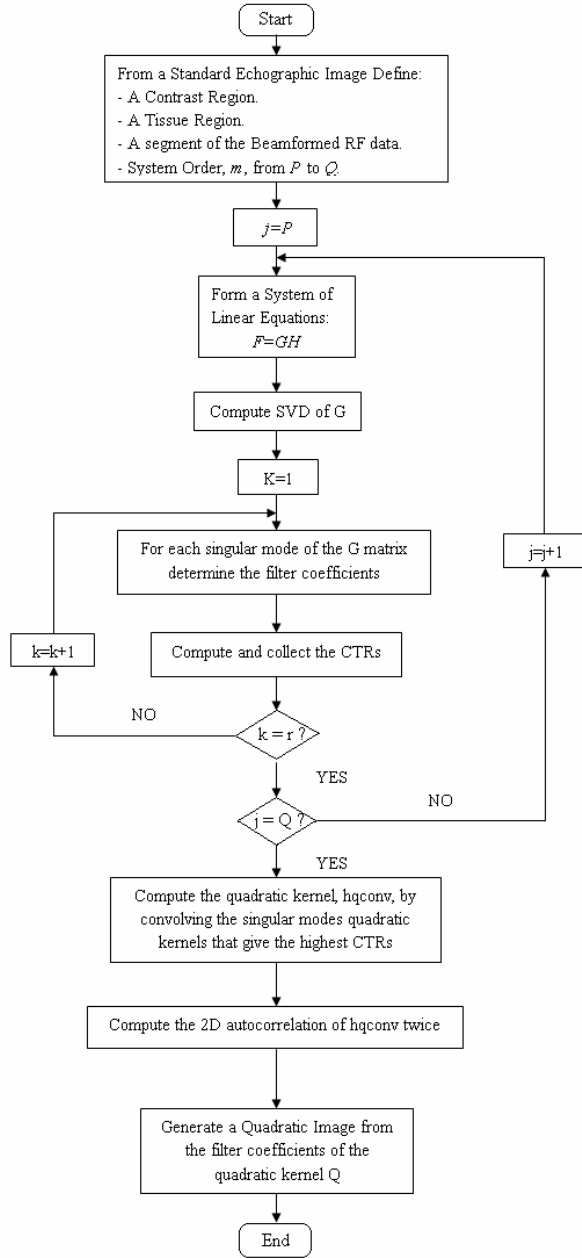


Fig.1 A flowchart of Quadratic image generation algorithm

3. MATERIALS AND METHODS

3.1 Experimental setup

We evaluated the algorithm with RF data acquired from experiments conducted *in vivo* on a juvenile pig. Bolus

injections of SonoVue™ (Bracco Research SA, Geneva, Switzerland), an UCA consisting of sulphur hexafluoride gas bubbles coated by a flexible phospholipidic shell, were administered with two different concentrations (0.01 mL/kg and 0.0025 mL/kg).

Three- and four-cycle pulses at 1.56 MHz were transmitted using a convex array probe (CA430E) with amplitude 3.8 V to scan a kidney. Technos MPX ultrasound system (ESAOTE S.p.A, Genova, Italy) was modified so that a pair of inverted pulses with the appropriate time delay was subsequently transmitted to produce images with the PI technique. In addition, in order to remove low frequency components due to tissue motion artifacts and retain harmonic frequency components from UCAs, RF data from PI imaging were filtered using the linear highpass filter with cutoff frequency 2.3 MHz. For each setup, three frames of RF data from the PI technique were collected with 10 s and 15 s delays after the injection of 0.01 mL/kg and 0.0025 mL/kg UCAs, respectively. RF data were acquired with 16-bit resolution at 20-MHz sampling frequency without TGC compensation and saved for off-line processing.

3.2 Contrast measurements

As a comparison of contrast enhancement between images from different techniques, we determine CTRs from data in the RF domain before scan converted. CTRs of images can be calculated with echoes from two referenced regions: First, the contrast region inside the kidney (bottom-left part). Second, the tissue region outside the kidney (on the left hand side of the contrast region with the same depth). Both regions are composed of 21 connected A-lines with 7.5-mm axial extent.

4. RESULTS AND DISCUSSION

Figure 2 shows images obtained using a standard B-mode image of the kidney after the injection of 0.01 mL/kg UCAs acquired using 3-cycle transmission, PI, Quadratic image from twice 2D correlation of 53th Singular mode, and Quadratic image from twice 2D correlation of the convolution of 49th & 53th Singular modes. Due to differences in dynamic ranges, each image is displayed with its full dynamic range as can be seen from the dB-level scale bars. Due to low microbubble populations in the perfused tissue of the kidney (Standard B-mode image), echogenicity from contrast regions is slightly lower than that from surrounding tissue regions, which agrees with the CTR value (-1.5178 dB) whereas the PI image provides CTR 14.3630 dB, echogenicity of the contrast region from the PI image appears brighter than that from surrounding tissue regions. Please note that the CTR value for the PI image without SH filtering was only 10.2319 dB, i.e. there is a 4.1311 dB gain due to the removal of tissue components introduced by motion. It is also worth noting that the SH image on the B-mode data suffers from significant loss in spatial resolution. The quadratic image from twice 2D correlation of 53th Singular mode provides CTR 22.3928 dB, which shows a contrast enhancement over both standard B-mode and PI images.

The quadratic image from twice 2D correlation of the convolution of 49th & 53th Singular modes is obtained using the

algorithm described by the flowchart of Figure 1 with the use of a 5.6-mm contrast A-line and a system order 15, provides CTR 27.4726 dB, which shows a contrast enhancement over the other three images.

We can clearly see not only the kidney's shape and boundary due to UCA echoes but also large vascular structures very similar to those seen in the PI, quadratic from twice 2D correlation of 53th Singular mode images. Also we can see that the kidney's shape and boundary due to UCA echoes are clearer in the Quadratic from twice 2D correlation of the convolution of 49th & 53th Singular modes image than that in the quadratic from twice 2D correlation of 53th Singular mode image. In addition, it can be seen that specular reflections of the quadratic images are as sharp as those from the PI image.

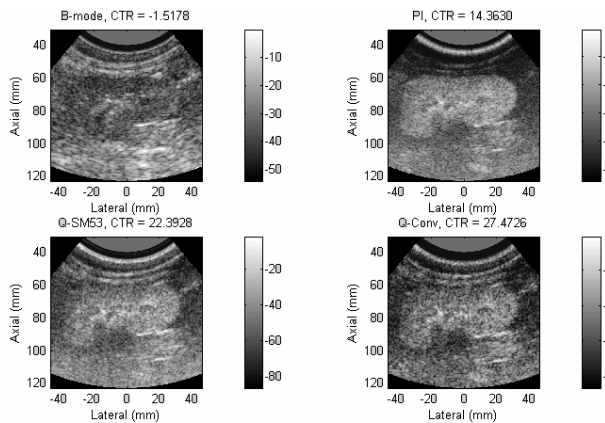


Fig. 2 Images of the: Standard B-mode image of the kidney at 10 s after the injection of 0.01 mL/kg, PI, Quadratic from twice 2D correlation of 53th Singular mode, and Quadratic from twice 2D correlation of the convolution of 49th & 53th Singular modes.

Fig. 3 shows the gray-level histograms produced from the Standard B-mode, PI, quadratic from twice 2D correlation of 53th Singular mode, and quadratic from twice 2D correlation of the convolution of 49th & 53th Singular modes images. In each case, the histogram from the UCA region is plotted with light solid line, while the histogram from tissue is plotted with darker solid line. One can see the degree of overlap between the histograms is highest for the standard B-mode image, whereas it is lowest for the quadratic from twice 2D correlation of the convolution of 49th & 53th Singular modes image.

5. CONCLUSIONS

We have proposed the new algorithm of post-beamforming second order Volterra filter (SOVF) for deriving the quadratic kernel based on the convolution of the singular modes quadratic kernels which give the highest CTRs to extract quadratic components from UCA nonlinear echoes with single transmission. Compared with the PI image processed from the same RF data, the quadratic images show comparable performance in terms of both contrast and spatial resolution. In addition, compared to PI

imaging, the VF approach does not require multiple transmissions for acquiring one image line. Therefore, this approach preserves the frame rate of the original B-mode system, an important advantage of ultrasound imaging over other medical imaging modalities.

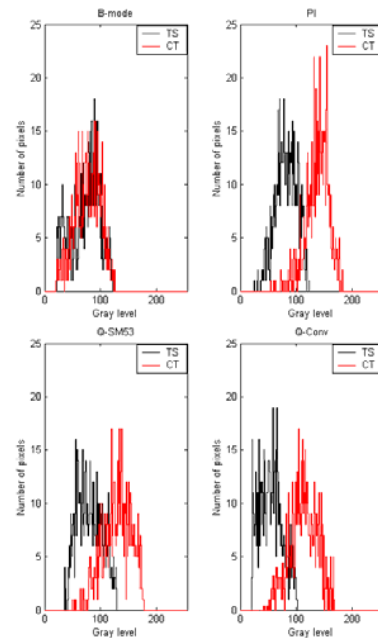


Fig. 3 Gray-level histograms produced from images shown in Fig. 2. Histograms are produced from the contrast region (lighter) and the tissue region (darker).

6. REFERENCES

- [1] D. H. Simpson, C. T. Chin, and P. N. Burns, "Pulse inversion Doppler: A new method for detecting nonlinear echoes from microbubble contrast agent," *IEEE Trans. Ultrason., Ferroelect., Freq. Contr.*, vol. 46, no. 2, pp. 372-382, Mar. 1999.
- [2] P. Phukpattaranont and E. S. Ebbini, "Post-beamforming second-order Volterra filter for nonlinear pulse-echo ultrasonic imaging," *IEEE Trans. Ultrason., Ferroelect., Freq. Contr.*, vol. 50, no. 8, pp. 987-1001, Aug. 2003.
- [3] P. Phukpattaranont, M. F. Al-Mistarihi and E. S. Ebbini, "Post-beamforming Volterra filters for contrast-assisted ultrasonic imaging: In-vivo results," in *Proc. IEEE Ultrason. Symp.*, 2003.